

**Original citation:**

Laory, Irwanda, Trinh, Thanh N., Smith, Ian F.C. and Brownjohn, James M.W.. (2014) Methodologies for predicting natural frequency variation of a suspension bridge. Engineering Structures, Volume 80 . pp. 211-221.

**Permanent WRAP URL:**

<http://wrap.warwick.ac.uk/66480>

**Copyright and reuse:**

The Warwick Research Archive Portal (WRAP) makes this work by researchers of the University of Warwick available open access under the following conditions. Copyright © and all moral rights to the version of the paper presented here belong to the individual author(s) and/or other copyright owners. To the extent reasonable and practicable the material made available in WRAP has been checked for eligibility before being made available.

Copies of full items can be used for personal research or study, educational, or not-for-profit purposes without prior permission or charge. Provided that the authors, title and full bibliographic details are credited, a hyperlink and/or URL is given for the original metadata page and the content is not changed in any way.

**Publisher's statement:**

© 2014, Elsevier. Licensed under the Creative Commons Attribution-NonCommercial-NoDerivatives 4.0 International <http://creativecommons.org/licenses/by-nc-nd/4.0/>

**A note on versions:**

The version presented here may differ from the published version or, version of record, if you wish to cite this item you are advised to consult the publisher's version. Please see the 'permanent WRAP URL' above for details on accessing the published version and note that access may require a subscription.

For more information, please contact the WRAP Team at: [wrap@warwick.ac.uk](mailto:wrap@warwick.ac.uk)

# 1 **Methodologies for predicting natural frequency variation of a suspension** 2 **bridge**

3 Irwanda Laory<sup>1</sup>, Thanh N. Trinh<sup>2</sup>, Ian F. C. Smith<sup>2</sup> and James M. W. Brownjohn<sup>3</sup>

4 *<sup>1</sup>School of Engineering, University of Warwick, Coventry, United Kingdom*

5 *Email: I.Laory@warwick.ac.uk*

6 *<sup>2</sup>Applied Applied Computing and Mechanic Laboratory, Swiss Federal Institute of*  
7 *Technology Lausanne (EPFL), Lausanne, Switzerland*

8 *<sup>3</sup>Vibration Engineering Section, College of Engineering, Mathematics and Physical Sciences,*  
9 *The University of Exeter, Exeter, United Kingdom*

## 12 **Abstract**

13 In vibration-based structural health monitoring, changes in the natural frequency of a structure  
14 are used to identify changes in the structural conditions due to damage and deterioration.  
15 However, natural frequency values also vary with changes in environmental factors such as  
16 temperature and wind. Therefore, it is important to differentiate between the effects due to  
17 environmental variations and those resulting from structural damage. In this paper, this task is  
18 accomplished by predicting the natural frequency of a structure using measurements of  
19 environmental conditions. Five methodologies - multiple linear regression, artificial neural  
20 networks, support vector regression, regression tree and random forest - are implemented to  
21 predict the natural frequencies of the Tamar Suspension Bridge (UK) using measurements  
22 taken from three years of continuous monitoring. The effects of environmental factors and  
23 traffic loading on natural frequencies are also evaluated by measuring the relative importance  
24 of input variables in regression analysis. Results show that support vector regression and  
25 random forest are the most suitable methods for predicting variations in natural frequencies.  
26 In addition, traffic loading and temperature are found to be two important parameters that  
27 need to be measured. Results show potential for application to continuously monitored  
28 structures that have complex relationships between natural frequencies and parameters such as  
29 loading and environmental factors.

30 **KEY WORDS:** *Environmental effect, artificial neural network, support vector regression,*  
31 *regression tree, random forest, variable importance, suspension bridge.*

32

### 33 **1. Introduction**

34 Many vibration-based approaches in structural health monitoring have been designed to  
35 identify changes in natural frequency values for the purpose of detecting changes in structural  
36 conditions that may indicate structural damage and degradation. In reality, however, civil  
37 engineering structures are subject to environment and operating effects caused by changes in  
38 temperature, traffic, wind, humidity and solar-radiation [1-5]. Such environmental effects also  
39 change natural frequency values, hence concealing changes due to structural damage [6-10].  
40 Therefore, it is important to distinguish between changes due to structural damage and  
41 changes resulting from environmental effects. This task is managed observing then modeling  
42 dependencies of natural frequencies on environmental parameters [11]. The prediction of  
43 natural frequencies of structures under environmental changes has been studied using methods  
44 such as linear regression analysis, artificial neural networks and support vector regression.

45 Multiple linear regression (MLR) was employed to predict changes in natural  
46 frequencies of the Alamosa Canyon Bridge (USA) due to environmental temperature variation  
47 [9] with natural frequencies formulated as a linear function of temperature data. It was found  
48 that the changes in the frequencies were linearly correlated with temperature taken from  
49 different locations on the bridge. Peeters et al. [12] conducted a one-year monitoring study for  
50 the Z24-Bridge (Switzerland) before it was deliberately damaged, applying a linear regression  
51 analysis to distinguish normal frequency changes from abnormal changes due to damage.  
52 Also, for this concrete box girder bridge, Peeters and Roeck [13] applied an autoregressive  
53 method with exogeneous inputs (ARX) to predict the bridge natural frequencies, where no  
54 relationship was found between natural frequencies and wind, rainfall and humidity. Liu and

55 Dewolf [3] simulated the varying natural frequencies under temperature changes using a  
56 linear regression analysis, concluding that the long-term variations of natural frequencies are  
57 closely related to the variation in in-situ concrete temperature for the three frequencies they  
58 measured. The MLR method has also been used to predict natural frequencies of suspension  
59 bridges and a footbridge using long-term monitoring data [11, 14].

60 Artificial neural networks (ANNs) have been successfully applied in fields such as  
61 pattern recognition [15], artificial intelligence [16] and civil engineering [17-20]. For long-  
62 term monitoring of structures, ANNs have been employed to predict time-dependent natural  
63 frequencies of a structure in order to eliminate the environmental effects on vibration-based  
64 damage detection procedures. For example, Ni et al. [21] applied an ANN to formulate the  
65 correlation between the natural frequencies and environmental temperatures taken from the  
66 cable-stayed Ting Kau Bridge (Hong Kong). Zhou et al [22] further investigated the  
67 performance of the ANNs formulated using the early stopping technique by constructing  
68 three different kinds of input, including mean temperatures, effective temperatures and  
69 principle components (PCs) of temperatures. The results indicated that when a sufficient  
70 number of PCs were taken into account, the ANN using temperature PCs as inputs predicted  
71 natural frequencies more accurately than that when using the mean temperatures. More  
72 studies on ANNs for the prediction of structural responses are found in references [22-25].

73 Support vector regression (SVR) is an application form of support vector machines that  
74 is a learning system using a high dimension feature space [26-27]. An attractive characteristic  
75 of SVR is that instead of minimizing the observed training error such as with MLR and  
76 ANNs, SVR involves minimizing the generalized error bound in order to achieve good  
77 performance. The generalized error bound is the combination of the training error and a  
78 regularization term that controls the complexity of prediction functions. A good overview of  
79 SVR is given in [28-29]. SVR has been successfully employed in fields such as text

80 categorization and pattern recognition as well as structural health monitoring [27, 30]. Ni et  
81 al. [31] applied SVR to predict natural frequencies of the cable-stayed Ting Kau Bridge  
82 (Hong Kong) subjected to temperature variations taken from one-year measurement data, the  
83 method exhibiting better prediction capability than the MLR method. Also using  
84 measurement data of this bridge, Hua et al. [32] combined principle component analysis  
85 (PCA) and SVR to simulate temperature-frequency correlations. It was found that the SVR  
86 method trained using the PCs of measured temperature data outperformed that trained using  
87 measured temperature data directly.

88         The methodologies used above are based on parametric functions that specify the form  
89 of the relationship between inputs and a response (output) but in many cases, the form of the  
90 relationship is unknown. Regression tree (R\_Tree) methods offer a non-parametric  
91 alternative [33] that has been used extensively in a variety of fields. The method has been  
92 found to be especially useful in biomedical and genetic research, speech recognition and other  
93 applied sciences [34]. Recent studies in the machine-learning field found that significant  
94 improvements in prediction accuracy have resulted from growing an ensemble of trees in a  
95 random way, a methodology called *random forest* (RF) [35]. It has been demonstrated that RF  
96 has improved prediction accuracy in comparison to other regression methods [36] but  
97 additionally provides measures of variable importance for each input variable [37-38]. This  
98 method has not been evaluated for its applicability to structural health monitoring, so this  
99 paper investigates the performance of RF on predicting natural frequencies through a case  
100 study of a suspension bridge.

101         The studies mentioned above have proposed methodologies for predicting the dynamic  
102 responses of bridges, but none has compared methodologies for prediction accuracy. This  
103 paper compares five methodologies – multiple linear regression, artificial neural networks,  
104 support vector regression, regression tree and random forest – in terms of their ability to

105 predict natural frequencies of a suspension bridge. Confidence intervals are then defined for  
106 the best method to differentiate the effects due to environmental changes from those caused  
107 by structural damage. Furthermore, the individual effects of temperature, wind and traffic  
108 loading on the natural frequency responses of the bridge are evaluated using the variable  
109 importance metric in regression analysis.

## 110 **2. Methodologies for predicting natural frequencies of the bridge**

### 111 *2.1. Multiple linear regression (MLR)*

112 Assuming that a response variable  $y$  (for example natural frequency) is linearly related  
113 to the  $p$  input variables (for example temperature, wind and traffic loading)  $x_1, \dots, x_p$  so that

$$114 \quad y = \beta_0 + \sum_{i=1}^p \beta_i x_i + e. \quad (1)$$

115 This relationship is known as a linear regression analysis, where  $\beta_i$  is the regression  
116 coefficient associated with the  $i^{\text{th}}$  input variable  $x_i$  and  $e$  the random error with mean zero  
117 and variance  $\sigma^2$ . Using the dataset of  $n$  observations in measurement time series, the  
118 unknown coefficients  $\beta_i$  are determined using the least-squares method.

### 119 *2.2. Artificial neural networks (ANNs)*

120 Artificial neural networks can be used as a nonlinear regression method to predict the  
121 natural frequency of a bridge. ANN is a two-stage regression in which the first stage is to  
122 create derived features  $Z_m$ , represented by hidden layer, from linear combinations of the  
123 inputs and the second stage is to model the output  $Y_m$  as a function of linear combinations of  
124 the  $Z_m$ .  $Z_m$  could be considered as a basis expansion of the original input  $X$ .

$$\begin{aligned}
Z_m &= \phi(\alpha_{0m} + \alpha_m^T X), m = 1, \dots, M, \\
T_k &= \beta_{0k} + \beta_k^T Z, k = 1, \dots, K, \\
f_k(X) &= T_k + e, k = 1, \dots, K,
\end{aligned} \tag{2}$$

126 where  $Z = (Z_1, Z_2, \dots, Z_M)$ ,  $\phi(v)$  is the activation function which is usually chosen to be the  
127 sigmoid  $\phi(v) = 1/(1 + e^{-v})$ ,  $e$  the random error,  $\alpha_i$  and  $\beta_i$  are unknown parameters. Given a  
128 training set  $\{x_i, y_i\}$  ( $i = 1, \dots, N$ ), the ANN regression model is formulated by searching these  
129 unknowns so that the sum-of-squared errors as a measure of fit reaches a minimum value.

$$R(\alpha, \beta) = \sum_{k=1}^K \sum_{i=1}^N (y_{ik} - f_k(x_i))^2 \tag{3}$$

131 The generic approach to minimizing,  $R(\alpha, \beta)$ , is by gradient descent, called back-  
132 propagation. A two-layer back-propagation neural network (BPNN) is employed to predict  
133 the natural frequencies of a structure. BPNN is first trained using the training set in order to  
134 formulate the relationship between the natural frequencies and environmental factors  
135 including direct loading such as traffic. BPNN is composed of one hidden layer and one  
136 output layer with a tan-sigmoid transfer function in the hidden layer and a linear transfer  
137 function in the output layer. The tan-sigmoid transfer function is capable of capturing the  
138 nonlinear relationship between input variables (in our example three of them) and output  
139 variables (in our example individual natural frequencies).

140 An important parameter to be determined when using BPNN for prediction tasks is the  
141 optimal number of hidden nodes in the hidden layer. A network with too few hidden nodes  
142 might not have enough flexibility to capture the nonlinearities in the relationship while a  
143 network with too many hidden nodes may have a tendency to overfit the training data.

144 2.3. *Support vector regression (SVR)*

145 The strategy of SVR is to transform nonlinear relationships from the original space into  
146 linear relationships in a new space (or feature space) defined using a kernel function so as to  
147 discover relationships more easily [27, 36]. The linear function in the new space is given by

148 
$$y(x) = w^T \varphi(x) + b + e \quad (4)$$

149 where  $w$  is the weight vector;  $b$  is the bias constant and  $\varphi(x)$  is the mapping function that  
150 transfers the input vector  $x$  into the new space. Given a training set  $\{x_i, y_i\}$  ( $i = 1, \dots, N$ ), a  
151 SVR model is obtained by minimizing the following objective function [39]

152 
$$\min_{w,b,e} J(w,e) = \frac{1}{2} w^T w + \frac{1}{2} \gamma \sum_{i=1}^N e_i^2 \quad (5)$$
  
subject to  $y_i = w^T \varphi(x_i) + b + e_i, \quad i = 1, \dots, N.$

153 where  $\gamma$  is the regularization parameter and  $e_i$  is the error. Such optimization that is subject  
154 to a condition is solved using the Lagrangian function

155 
$$L(w,b,e,\alpha) = J(w,e) - \sum_{i=1}^N \alpha_i \{w^T \varphi(x_i) + b + e_i - y_i\} \quad (6)$$

156 where  $\alpha_i$  is a Lagrange multiplier. The conditions for optimality are given by

$$\begin{cases}
\frac{\partial L}{\partial w} = 0 \rightarrow w = \sum_{i=1}^N \alpha_i \varphi(x_i) \\
\frac{\partial L}{\partial b} = 0 \rightarrow \sum_{i=1}^N \alpha_i = 0 \\
\frac{\partial L}{\partial e} = 0 \rightarrow \alpha_i = \gamma e_i, & i = 1, \dots, N. \\
\frac{\partial L}{\partial \alpha} = 0 \rightarrow w^T \varphi(x_i) + b + e_i - y_i = 0, & i = 1, \dots, N.
\end{cases} \quad (7)$$

Elimination of  $w$  and  $e$  yields a set of linear equations that are written in the matrix form

$$\begin{bmatrix} 0 & 1_N^T \\ 1_N & \Omega + \gamma^{-1} I_N \end{bmatrix} \begin{bmatrix} b \\ \alpha \end{bmatrix} = \begin{bmatrix} 0 \\ Y \end{bmatrix} \quad (8)$$

where  $Y = [y_1, \dots, y_N]^T$ ,  $1_N = [1, \dots, 1]^T$  and  $\alpha = [\alpha_1, \dots, \alpha_N]^T$ .  $I_N$  is an  $N \times N$  identity matrix and  $\Omega$  is a  $N \times N$  kernel matrix defined by a kernel function as

$$\Omega_{ij} = \varphi(x_i)^T \varphi(x_j) = K(x_i, x_j). \quad (9)$$

The kernel function is designed to compute inner-products in the new space using only the original input data. The choice of  $K$  implicitly determines  $\varphi$  and the new space. Thus, the advantage of kernel functions is that if a kernel function  $K$  is given, it is not necessary to know the explicit form of the mapping function  $\varphi(x)$ . The selection of the kernel function generally depends on the application domain. It has been shown that Gaussian radial-basis function (RBF) is a reasonable first choice of kernel functions since it has only a single parameter (standard deviation,  $\sigma$ ) to be determined [27, 40]. The Gaussian RBF is expressed as

171 
$$K(x_i, x_j) = e^{-\|x_i - x_j\|^2 / 2\sigma^2}. \quad (10)$$

172 Solving Equation (8) identifies the values of  $\alpha$  and  $b$ . Then, substituting these values into  
173 Equation (4) leads to the prediction

174 
$$y(x) = \sum_{i=1}^N \alpha_i K(x, x_i) + b. \quad (11)$$

175 There are only two tuning parameters,  $\gamma$  and  $\sigma$ , that need to be determined when using the  
176 RBF kernel function and their optimal values are determined using the grid search method .  
177 Possible intervals for the two parameters are first defined. Then all grid points are tried to find  
178 the one giving the best accuracy. For each combination of the two parameters, SVR is trained  
179 using the training data and their performance is evaluated by a ten-fold cross-validation  
180 scheme.

#### 181 2.4. Regression tree (*R\_Tree*)

182 Regression tree is a nonparametric statistical method [33] that offers an alternative to  
183 parametric regression methods which usually require assumptions and simplifications to form  
184 the relationship. A regression tree is built by recursively partitioning the entire dataset,  
185 represented by a *root node*, into more homogeneous groups with each to be represented by a  
186 node. When the splitting process terminates, each resulting group is referred to as a terminal  
187 node. Splitting at each node is based on one value of an input variable that leads to the most  
188 homogeneous resulting nodes. Assuming that we have a partition into  $M$  regions  $R_1, R_2, \dots,$   
189  $R_M$  the system model is identified as

190 
$$y(x) = \text{ave}(y_j | x_j \in R_m) + e \quad (11)$$

191 Where  $y_j$  and  $x_j$  represent the response and input variables at  $j^{th}$  observation respectively.  
 192 Equation 10 shows that the predicted response is the average of  $y_j$  in region  $R_m$  with the  
 193 error  $e$ .

194 A simple regression tree is built with two input variables  $x_1$  and  $x_2$  and a response  $y$   
 195 by considering a recursive partition as shown in Figure 1(a). First, we select the *splitting*  
 196 *variable* (for example,  $x_1$ ) and the *split point* (for example  $s_1$ ) in order to achieve the most  
 197 homogeneous splitting groups and split the space of the dataset into two groups. The selected  
 198 variable and point solve

$$199 \quad \min_{j,s} \left[ \sum_{x_i \in R_1(j,s)} (y_i - c_1)^2 + \sum_{x_i \in R_2(j,s)} (y_i - c_2)^2 + \right] \quad (11)$$

200  $c_1$  and  $c_2$  are the mean value of all the responses in the corresponding groups. Then, each of  
 201 these groups is further split into two more groups. As shown in Figure 1(a), the group  $x_1 \leq s_1$   
 202 is split at  $x_2 \leq s_2$  and finally the group  $x_1 > s_1$  is split at  $x_1 = s_3$ . The process results in four  
 203 groups  $R_1, \dots, R_4$ . This process can be represented by the binary tree (Figure 1(b)). The  
 204 entire dataset sits at the top of the tree, as a so-called root node. Observations (data points)  
 205 satisfying the condition at each node are assigned to the left branch, and the others to the right  
 206 branch. The terminal nodes of the tree correspond to the groups,  $R_1, \dots, R_4$ . Once a tree has  
 207 been built, the response for any new observation can be predicted by following the path from  
 208 the root node down to the appropriate terminal node of the tree, based on the observed values  
 209 of the splitting variables.

210 When determining tree size, note that a small tree may not capture a nonlinear  
 211 relationship that may exist while a very large tree may over-fit the data. Therefore, tree size is  
 212 a tuning parameter and the optimal tree size should be adaptively chosen from the data. The

213 preferred strategy is to gradually increase the tree size and evaluate the accuracy of each tree  
214 size until each node contains fewer than a given number of observations (for example, 5).  
215 Then this large tree is pruned by sequentially cutting off branches that add the smallest  
216 capability to predictive performance of the tree according to a specified pruning criterion.

## 217 2.5. *Random forest (RF)*

218 A random forest is a combination of regression trees that are grown in random ways  
219 [35]. The idea behind the random forest method is to generate an ensemble of low-correlated  
220 regression trees and average results in order to reduce variance. The low-correlated trees are  
221 generated by adding randomization in two steps: (i) each tree is grown using a random sub-  
222 dataset of observations and (ii) each node of a tree is split using a random subset of input  
223 variables. Figure 2 shows the layout of the random forest method.

224 The first step is to generate  $B$  sub-datasets of observations by randomly copying  
225 observations from the original training set  $L$  until each sub-dataset has the same number of  
226 observations  $N$  as the original training set. Some observations can be chosen several times  
227 for each sub-dataset, whereas others are not chosen at all. It has been proved that about 37%  
228 of the observations in the original training set are not chosen for each sub-dataset [38, 41].  
229 The collection of non-chosen observations corresponding to each sub-dataset functions as a  
230 validation set. Each sub-dataset is denoted  $L_b$  where  $b = 1, 2, \dots, B$ .

231 The second step involves growing a regression tree ( $T_b$ ) using a sub-dataset ( $L_b$ ). This  
232 step is to reduce further the correlation between the regression trees that enter into the  
233 averaging step later. This is achieved during the tree-growing process by randomly selecting  
234 a subset of  $m$  input variables from all  $p$  input variables ( $m \leq p$ ) before splitting each node.  
235 A regression tree is grown by recursively repeating the following three sub-steps for each  
236 node until the specified number of observations within each node is reached.

237 - Randomly select a subset of  $m$  variables from all  $p$  variables.

238 - Find the best split among the  $m$  variables.

239 - Split the selected node into two resulting nodes.

240 After  $B$  regression trees are grown from  $B$  sub-datasets, an ensemble of these  $B$  trees  
241 is called a random forest. The random forest makes a prediction for a new observation  $x$  by  
242 using each regression tree  $T_b$  in the forest to obtain a prediction  $y_b(x)$  and then averaging  $B$   
243 prediction values from the  $B$  trees:

$$244 \quad y(x) = \frac{1}{B} \sum_{b=1}^B y_b(x) + e \quad (12)$$

### 245 3. Case study subject: The Tamar suspension bridge

246 The Tamar Suspension Bridge, as shown in Figure 3, is a road bridge connecting  
247 Saltash to Plymouth in southwest England. The original bridge was designed as a  
248 conventional suspension bridge with symmetrical geometry and was first opened in 1961. The  
249 total length is 642 m with a main span of 335 m and side spans of 114 m and the tower height  
250 is 73 m. Trusses are 4.9 m deep with chords of welded hollow box structures. To meet the  
251 requirement that bridges should be capable of carrying lorries up to 40 tons, the Tamar Bridge  
252 was strengthened and widened in March 1999 and the upgrading was completed in December  
253 2001[42-43]. The upgrading included replacing the original composite main deck by a three-  
254 lane orthotropic steel deck, adding single lane cantilevers at each side of the truss and  
255 installing sixteen new cables acting as additional stays to carry the additional dead load of  
256 new cantilever lanes and associated temporary works. Figure 4 shows the layout of one of the  
257 truss sections with the main orthotropic deck and two cantilever lanes.

258 Many types of sensors were installed during and subsequent to the strengthening and  
259 widening to monitor the behavior of the bridge [44]. They included anemometers,

260 displacement sensors, thermometers, load cells and accelerometers. Most recently, a robotic  
261 total station was added to monitor the deflection of the bridge deck and a pair of  
262 extensometers installed to track relative movement across the single expansion joint located  
263 around the Saltash Tower [45]. Measurement data have been collected continuously since  
264 February 2007.

265 These data used in this study include air temperature, wind velocity, the measured  
266 natural frequencies of the bridge and the number of vehicles crossing the bridge every hour.  
267 Vehicle crossing data were available from the bridge toll reports, temperature and wind values  
268 are 30-minute averages of data sampled at either 1Hz from four thermistors on the cable and  
269 deck and an anemometer close to midspan, while frequencies are derived from modal analysis  
270 of 64-Hz sampled acceleration signals from a pair of accelerometers located near mid span.  
271 Locations of these sensors are shown in Figure 5. The covariance-driven stochastic subspace  
272 identification (SSI-COV) procedure operated automatically on the acceleration data after 8-  
273 fold decimation, reporting frequency and damping estimates at 30 minute intervals.

274 Figure 6 shows the time history of air temperature for three years, including daily and  
275 seasonal temperature variations. The temperature ranges from -5 °C to 25 °C between winter  
276 and summer. The first five natural frequencies of the bridge are summarized in Table 1.

#### 277 **4. Results**

278 The five regression methodologies presented in the previous section are applied to  
279 predict the natural frequency variation of the Tamar Bridge based on environmental factors as  
280 well as traffic loading. The prediction is performed for each natural frequency separately. The  
281 measurement data taken from July 2007 to January 2010 on the Tamar Bridge are divided into  
282 two non-overlapping and independent data sets: a training set of 70% and a test set of 30%.  
283 While the training set (from July 2007 to May 2009) is used for regression analysis to predict

284 natural frequencies, the test set is used for assessing prediction accuracy (from June 2009 to  
285 January 2010).

#### 286 4.1. *Multiple linear regression*

287 The relationship between natural frequency responses and air temperature, wind and  
288 traffic loading are first formulated for each frequency using the least square method. Figure 7  
289 shows the prediction of the 10-day time histories (from 20 to 30 July 2009) of the third  
290 frequency that is compared with the measured frequency in the test phase. This figure  
291 indicates that the predicted frequency is unable to capture the high variation in the natural  
292 frequency. Table 2 presents the mean square error (MSE) values in the training and test sets,  
293 where the error is the difference between the measured frequency value and its corresponding  
294 predicted value. For frequency 1 and 3, MSE values in the training set are somewhat larger  
295 than those in the test set. This is because there are more outliers in the training data than in  
296 the test set.

#### 297 4.2. *Artificial neural networks*

298 The optimal number of hidden nodes in the hidden layer is determined so that the  
299 validation error reaches the minimum value. To do this, a set of neural networks with respect  
300 to the increasing number of hidden nodes from 1 to 50 are trained using training data. The  
301 number of hidden nodes of the neural network that gives the minimum error is taken as the  
302 optimal number.

303 Table 3 presents the optimal numbers of hidden nodes for five natural frequencies,  
304 together with MSE values of the training set and the test set. The optimal number of hidden  
305 nodes for five frequencies ranges from 10 to 33 nodes. These values are close to the optimal  
306 value (19 hidden nodes) for the first natural frequency of the Ting Kau cable-stayed bridge  
307 [46]. Figure 8 shows the predicted natural frequency along with the measured frequency.  
308 Comparing Figure 7 and Figure 8 indicates that an artificial neural network achieves a better

309 prediction value than multiple linear regression. Comparing the prediction capability of ANN  
310 with other methods is further discussed in Section 4.6.

#### 311 4.3. Support vector regression

312 Table 4 presents the optimal values of  $\gamma$  and  $\alpha$  that give the best performance (lowest  
313 MSE) of SVR for five natural frequencies. The corresponding MSEs are also listed in this  
314 table. Comparing the MSE values in Table 4 with Table 2 and Table 3 indicates that the SVR  
315 method has a better performance than the MLR and ANN methods in both the training set and  
316 the test set. For example, the prediction error (in the test set) for frequency 5 using SVR is  
317 reduced by 20% when compared with the prediction error using MLR. Figure 9 shows the  
318 predicted and measured time histories of frequency 3 from July 20 to 30, 2009. It is shown  
319 that the predicted frequencies closely match the measured ones.

#### 320 4.4. Regression tree

321 Figure 10 shows the mean squared error with respect to the increasing number of  
322 terminal nodes (i.e. tree size) of the pruned tree for the first natural frequency. The optimal  
323 tree size (i.e. the point where increasing tree size only leads to minor decrease of MSE) for  
324 this frequency is composed of 31 terminal nodes. The optimal tree sizes for the second and  
325 third frequencies are 44 and 35 terminal nodes respectively (Table 5). It is observed that the  
326 higher frequency requires more terminal nodes, leading to a larger tree size, i.e. higher tree  
327 complexity. Table 5 also presents the mean squared errors in the training and test sets. The  
328 prediction of the R\_Tree method is better than that of the ANN and MLR methods but it is not  
329 as good as that of the SVR method.

330 Figure 11 shows the 10-day time histories of measured and predicted frequencies from  
331 July 20 to July 30, 2009. For both sets, the predicted frequency time history reasonably  
332 matches the measured one. Flatness exists at some peaks of the predicted time history. This

333 is because the observations at the peaks fall into the same groups where the predicted  
334 responses are equal to the mean of measured responses within the corresponding group.

#### 335 4.5. *Random forest*

336 When applying the random forest method for regression analysis, three parameters need  
337 to be determined: (i) the sufficient number  $B$  of trees, (ii) the optimal number of observations  
338 in each terminal node and (iii) the number  $m$  of input variables randomly chosen as  
339 candidates for splitting at each node. For the Tamar Bridge, there are three input variables (i.e.  
340  $p = 3$ ) including temperature, wind and traffic. For this case study, to reduce the correlation  
341 between regression trees, the number of input variables chosen for splitting at each node is 2  
342 (i.e.  $m = 2$ ).

343 Figure 12 shows that when the number of trees increases, the mean squared error  
344 computed from the validation set decreases. The prediction is stable at about 100 trees for  
345 both cases of 1 and 50 observations in each terminal node. It is seen that the tree with 50  
346 observations in terminal nodes performs better than that with only one observation in terminal  
347 nodes. This is attributable to the over-fitting situation when growing a tree to its maximum  
348 size (i.e. one observation in terminal nodes).

349 Figure 13 shows the change in the normalised mean squared error with respect to the  
350 increase in the number of observations in terminal nodes for 5 frequencies. For each  
351 frequency, the normalised MSE is calculated by dividing the MSE by the difference between  
352 maximum and minimum MSE. When the number of observations in terminal nodes starts  
353 increasing, initially the normalised MSE of all five frequencies drops dramatically to a  
354 minimum and then it increases gradually. The optimal number of observations in terminal  
355 nodes ranges from 10 to 50 observations. Table 6 presents the optimal number of  
356 observations for each frequency together with its mean squared errors computed from the  
357 training set and the test set. The results show that the random forest method has the smallest

358 errors as compared with those from the previous four methods. Figure 14 compares the  
359 predicted natural frequency with the measured frequency. The predicted frequency closely  
360 matches the measured one.

#### 361 *4.6. Performance comparisons and discussions*

362 In order to find a suitable method to predict the natural frequency responses from  
363 environmental measurement data for a suspension bridge, the prediction capability of five  
364 regression methods are compared. The result of a regression method can have a very good fit  
365 to the training data; however, it may poorly predict the response for a new observation. Thus,  
366 the prediction capability of these methods is evaluated through prediction error that is defined  
367 as the mean squared error from the test set, with a smaller prediction error indicating a better  
368 prediction capability. When comparing the prediction error of the five regression methods  
369 from Table 2 to Table 6, it can be seen that the four nonlinear regression methods (ANNs,  
370 SVR, R\_Tree and RF) predict frequencies more accurately than the MLR method. Table 7  
371 presents the reduction in the prediction error for these methods when using the prediction  
372 error of the MLR method as a basis. For frequency 5, SVR and RF can reduce the prediction  
373 error up to 20% when compared with MLR. The good performances of SVR and RF indicate  
374 the possibility of existence of non-linear correlations between natural frequency responses and  
375 environmental factors as well as traffic loading for the Tamar Suspension Bridge. In addition,  
376 comparing Figure 11 and Figure 14 demonstrates that RF employing multiple trees, which are  
377 grown in a random way, can lead to better predictions than the R\_Tree method that employs a  
378 single tree. RF is able to capture the high variations at peaks of frequency time histories.

379 The performance of SVR and RF are further assessed through a normality test [47].  
380 From a statistical point of view the error, which is the difference between the predicted value  
381 and the corresponding measured frequency value, complies with a normal distribution with  
382 zero mean [32]. Figure 15 compares the observed probability density functions of the error

383 with the corresponding theoretical curves of the normal distribution obtained using the mean  
384 and standard deviation values computed from error values. The figure shows the observed  
385 probability distribution of the error for SVR and RF methods is in good agreement with a  
386 normal distribution with zero mean.

387 SVR and RF are used to define the confidence intervals around the predicted natural  
388 frequencies for a new observation. It is found that the error in the training data for SVR and  
389 RF also have a normal distribution with zero mean. Thus, the confidence interval is defined  
390 based on the error variance of the training data. Figure 16 shows the identified and predicted  
391 natural frequencies for RF between July 20 and July 30 (2009), together with the 95%  
392 confidence interval for the second natural frequency. For the test set, the ratio of the data that  
393 falls within the 95% confidence level to the full set of the data is referred to as the success  
394 rate. For SVR, the success rates for frequencies 1 to 5 are 98%, 91%, 98%, 94% and 91%,  
395 respectively. The corresponding success rates for RF are 98%, 91%, 98%, 94% and 89%.  
396 These high success rates indicate that the variations in bridge natural frequencies can be  
397 accounted for by measuring temperature, wind and traffic loading. These rates also  
398 demonstrate the consistency of continuously monitored data from 2007 to 2010, thereby  
399 establishing a baseline data for continuous health monitoring of the bridge. In addition, the  
400 success rate can be used as a damage-detection index. If the success rates for future natural  
401 frequencies change, it is likely that the bridge has experienced some kind of structural change.

## 402 **5. Effects of environmental factors and traffic loading on natural frequencies of the** 403 **bridge**

404 The changes in bridge natural frequencies are adequately accounted for by three factors:  
405 temperature, wind and traffic loading. This study identifies the degree to which each factor  
406 has an effect on the frequency change. Simultaneous effects of these factors on the first five  
407 natural frequency responses are evaluated. This is carried out by using the measure of relative

408 importance of input variables in regression analysis. The measure of relative importance  
409 indicates the variables that are highly related to the response for interpretation purposes.

#### 410 *5.1. Evaluation of effects using relative importance metrics of the multiple linear regression* 411 *method*

412 Multiple linear regression can be used to evaluate the contribution of an individual input  
413 variable  $x_j (j = 1, \dots, p)$  to the prediction of a response  $y$ . The contribution of each variable is  
414 compared with that of other variables using a metric of so-called relative importance. Several  
415 relative importance metrics have been proposed to assess the amount of variation in the  
416 response that is explained by each individual variable [48-49]. In this study, since the  
417 correlation between input variables is negligible, the relative importance of each individual  
418 variable is defined as the squared correlation coefficient of an input variable  $x_j$  with the  
419 response  $y$ .

420 Figure 17 shows the relative importance of temperature, wind and traffic loading using  
421 MLR for the first five natural frequencies of the bridge. The effects of temperature, wind and  
422 traffic loading on the first frequency are 8%, 18% and 74%. Such effects correspond to 34%,  
423 10% and 56% for the second frequency. They are 28%, 10% and 62% for the third frequency  
424 and 22%, 10% and 68% for the fifth frequency. Except for the fourth frequency (i.e. 70%,  
425 21% and 9%), based on relative importance metrics defined using MLR, traffic loading is the  
426 main factor that affects the natural frequencies.

#### 427 *5.2. Evaluation of effects using relative importance metrics of the random forest method*

428 The random forest method has improved the prediction accuracy in comparison to other  
429 prediction methods. Besides, RF also evaluates the relative importance of variables in a  
430 dataset in order to measure the prediction strength of each variable.

431 As mentioned in Section 2.5, approximately 63% of the observations in the original  
432 training set are used for each sub-dataset on which to grow each individual tree. The non-

433 chosen observations (about 37%) are utilized as validation observations for that tree. The  
 434 computation of the importance of an input variable  $x_j$  is carried out one tree at a time. First,  
 435 when the  $b^{\text{th}}$  tree  $T_b$  is grown, the validation observations are then used to determine the mean  
 436 squared error from the validation data  $MSE_b$ . Next, the values of variable  $x_j$  in the validation  
 437 data are randomly permuted while leaving the values of all other variables unchanged. Then,  
 438 the permuted observations are used in the tree  $T_b$  and the mean squared error from the  
 439 permuted validation data  $MSE_b(x_j)$  is computed. If  $x_j$  is important, permuting its observed  
 440 values will reduce the prediction accuracy of each observed value in the validation data. Thus,  
 441  $MSE_b(x_j)$  from the permuted validation data is larger than  $MSE_b$  from the un-permuted  
 442 data.

443 Finally, a measure of the importance of the  $j^{\text{th}}$  variable  $x_j$  is obtained by averaging the  
 444 mean squared errors from the permuted validation data over all of the trees:

$$445 \quad \text{imp}(x_j) = \frac{1}{B} \sum_{b=1}^B (MSE_b(x_j) - MSE_b). \quad (13)$$

446 The relative importance of each variable is computed by normalizing its importance to  
 447 the summation of the importance of all variables. The relative importance metrics are  
 448 expressed in percentage. Figure 18 shows the relative importance of temperature, wind and  
 449 traffic loading on the natural frequency responses of the bridge. There is a significant effect  
 450 of traffic loading on the frequency. Figure 18 also indicates that while the effect of traffic  
 451 loading decreases from frequencies 1 to 5, the effect of temperature increases respectively.  
 452 Both effects are almost similar for frequency 5 and the effect of temperature is more dominant  
 453 than that of traffic loading for frequency 4.

### 454 5.3. Discussion

455 Comparing Figure 17 and Figure 18 shows that although variable importance metrics  
456 are defined in two different ways using multiple linear regression and random forest, the  
457 importance rankings for temperature, wind and traffic are identical. For the first frequencies,  
458 the averaged percentages of the effects taken from both variable importance metrics are about  
459 8%, 17% and 75% respectively. Such percentages correspond to 26%, 15% and 59% for the  
460 second frequency, 24%, 9% and 66% for the third frequency, 60%, 22% and 18% for the  
461 fourth frequency and 31%, 11% and 58% for the fifth frequency. A possible reason for the  
462 effect of traffic loading is that there is a significant contribution of the traffic mass to the total  
463 mass of the truss-span suspension bridge. Despite the strong influence on other frequencies,  
464 the relative effect of the traffic on the fourth frequency is quite small. This could be due to the  
465 fact that the fourth frequency refers to a torsional vibration mode while other frequencies refer  
466 to vertical and lateral modes.

467 As for temperature effects, the influence on the variation of the fourth and fifth  
468 frequencies is larger than that of the other frequencies. This could be caused by the non-linear  
469 temperature distribution due to solar radiation. In general, for successful data interpretation  
470 when monitoring natural frequency responses of suspension bridges, the effects of both traffic  
471 loading and temperature need to be taken into account.

## 472 6. Conclusions

473 This paper compares five methodologies to predict the natural frequency responses of a  
474 suspension bridge using measurements of temperature, wind and traffic loading. The  
475 following conclusions are drawn

- 476 • Random forest and support vector regression are the most appropriate methods for  
477 predicting the natural frequencies of a suspension bridge using measurement data of  
478 temperature, wind and traffic loading. This may be due to non-linear behavior.

- 479 • The relative importance of input variables of regression analysis is a useful metric to  
480 evaluate the simultaneous effects of environmental factors and traffic loading on the  
481 long-term natural frequency responses of a bridge.
- 482 • Traffic loading and temperature are the most influential parameters on natural frequencies  
483 of the suspension bridge studied. Obtaining these parameters should be a priority when  
484 using natural frequency changes to detect damage.

## 485 **Acknowledgements**

486 The authors are grateful to Dr. Minh-Hai Pham and Dr. Ki-Young Koo for their contributions  
487 to this research.

## 488 **References**

- 489 [1] Wahab MA, De Roeck G. Effect of temperature on dynamic system parameters of a highway  
490 bridge. *Structural Engineering International*. 1997;7:266-70.
- 491 [2] Yuen K-V, Kuok S-C. Ambient interference in long-term monitoring of buildings. *Engineering*  
492 *Structures*. 2010.
- 493 [3] Liu C, DeWolf JT. Effect of temperature on modal variability of a curved concrete bridge under  
494 ambient loads. *Journal of Structural Engineering*. 2007;133:1742-51.
- 495 [4] Xu Z-D, Zhishen Wu. Simulation of the effect of temperature variation on damage detection in a  
496 long-span cable-stayed bridge. *Structural Health Monitoring*. 2007;6:177-89.
- 497 [5] Brownjohn JM. Thermal effects on performance on tamar bridge. in *4th International*  
498 *Conference on Structural Health Monitoring of Intelligent Infrastructure (SHMII-4)*. Zurich,  
499 Switzerland. 2009.
- 500 [6] Laory I, Trinh TN, Smith IFC. Evaluating two model-free data interpretation methods for  
501 measurements that are influenced by temperature. *Adv Eng Inform*. 2011;25:495-506.
- 502 [7] Posenato D, Lanata F, Inaudi D, Smith IFC. Model-free data interpretation for continuous  
503 monitoring of complex structures. *Advanced Engineering Informatics*. 2008;22:135-44.
- 504 [8] Posenato D, Kripakaran P, Inaudi D, Smith IFC. Methodologies for model-free data  
505 interpretation of civil engineering structures. *Computers & Structures*. 2010;88:467-82.
- 506 [9] Sohn H, Dzwonczyk M, Straser EG, Kiremidjian AS, Law K, Meng T. An experimental study  
507 of temperature effect on modal parameters of the alamosa canyon bridge. *Earthquake*  
508 *Engineering and Structural Dynamics*. 1999;28:879-97.
- 509 [10] Trinh TN, Koh CG. An improved substructural identification strategy for large structural  
510 systems. *Structural Control and Health Monitoring*. 2011;doi: 10.1002/stc.463.
- 511 [11] Moser P, Moaveni B. Environmental effects on the identified natural frequencies of the dowling  
512 hall footbridge. *Mechanical Systems and Signal Processing*. 2011;25:2336-57.
- 513 [12] Peeters B, Maeck J, Roeck GD. Vibration-based damage detection in civil engineering:  
514 Excitation sources and temperature effects. *Smart Materials and Structures*. 2001;10:518.

- 515 [13] Peeters B, De Roeck G. One-year monitoring of the Z24-bridge: Environmental effects versus  
516 damage events. *Earthquake Engineering & Structural Dynamics*. 2001;30:149-71.
- 517 [14] Yang D, Youliang D, Aiqun L. Structural condition assessment of long-span suspension bridges  
518 using long-term monitoring data. *Earthquake Engineering and Engineering Vibration*.  
519 2010;9:123-31.
- 520 [15] Bishop C. *Neural networks for pattern recognition*: Oxford University Press, USA; 1996.
- 521 [16] Raphael B, Smith IFC. *Fundamentals of computer-aided engineering*: West Sussex, England :  
522 Wiley; 2003.
- 523 [17] Chan THT, Ni YQ, Ko JM. Neural network novelty filtering for anomaly detection of tsing ma  
524 bridge cables in *The 2nd International Workshop on Structural Health Monitoring*. Stanford  
525 University, Stanford, CA, USA. 1999.
- 526 [18] Fernandez B, Parlos AG, Tsai WK. Nonlinear dynamic system identification using artificial  
527 neural networks (anns). New York, NY, USA: IEEE. 1990.
- 528 [19] Huang C-C, Loh C-H. Nonlinear identification of dynamic systems using neural networks.  
529 *Computer-Aided Civil and Infrastructure Engineering*. 2001;16:28-41.
- 530 [20] Adeli H. *Neural networks in civil engineering: 1989–2000*. *Computer-Aided Civil and*  
531 *Infrastructure Engineering*. 2001;16:126-42.
- 532 [21] Ni YQ, Zhou HF, Ko JM. Generalization capability of neural network models for temperature-  
533 frequency correlation using monitoring data. *J Structural Engineering*. 2009;135:1290.
- 534 [22] Zhou HF, Ni YQ, Ko JM. Constructing input to neural networks for modeling temperature-  
535 caused modal variability: Mean temperatures, effective temperatures, and principal components  
536 of temperatures. *Engineering Structures*. 2010;32:1747-59.
- 537 [23] Zhou HF, Ni YQ, Ko JM. Performance of neural networks for simulation and prediction of  
538 temperature-induced modal variability. in *Smart Structures and Materials 2005: Sensors and*  
539 *Smart Structures Technologies for Civil, Mechanical, and Aerospace Systems, 7 March 2005*.  
540 USA: SPIE-Int. Soc. Opt. Eng. 2005.
- 541 [24] Freitag S, Graf W, Kaliske M, Sickert JU. Prediction of time-dependent structural behaviour  
542 with recurrent neural networks for fuzzy data. *Computers & Structures*. In Press, Corrected  
543 Proof.
- 544 [25] Graf W, Freitag S, Sickert J-U, Kaliske M. Prediction of time-dependent structural behavior  
545 with recurrent neural networks. in *The Sixth International Structural Engineering and*  
546 *Construction Conference*. Zürich, Switzerland. 2011. 789-94.
- 547 [26] Vapnik V, Golowich S, Smola A. Support vector method for function approximation, regression  
548 estimation, and signal processing. in *Advances in Neural Information Processing Systems 9*.  
549 1996.
- 550 [27] Saitta S, Kripakaran P, Raphael B, Smith IFC. Feature selection using stochastic search: An  
551 application to system identification. *Journal of Computing in Civil Engineering*. 2010;24:3-10.
- 552 [28] Smola AJ, Schölkopf B. A tutorial on support vector regression. *Statistics and Computing*.  
553 2004;14:199-222.
- 554 [29] Basak D, Pal S, Patranabis D. Support vector regression. *Neural Information Processing –*  
555 *Letters and Reviews*. 2007;11.
- 556 [30] Zhang J, Sato T. Experimental verification of the support vector regression based structural  
557 identification method by using shaking table test data. *Structural Control and Health*  
558 *Monitoring*. 2008;15:505-17.

- 559 [31] Ni YQ, Hua XG, Fan KQ, Ko JM. Correlating modal properties with temperature using long-  
560 term monitoring data and support vector machine technique. *Engineering Structures*.  
561 2005;27:1762-73.
- 562 [32] Hua XG, Ni YQ, Ko JM, Wong KY. Modeling of temperature-frequency correlation using  
563 combined principal component analysis and support vector regression technique: ASCE; 2007.
- 564 [33] Breiman L, Friedman J, Stone C, Olshen RA. *Classification and regression trees*: Chapman &  
565 Hall/CRC; 1984.
- 566 [34] Izenman A. *Modern multivariate statistical techniques : Regression, classification, and manifold  
567 learning*: Springer New York; 2008.
- 568 [35] Breiman L. Random forests. *Machine Learning*. 2001;45:5-32.
- 569 [36] Zheng L, Watson DG, Johnston BF, Clark RL, Edrada-Ebel R, Elseheri W. A chemometric  
570 study of chromatograms of tea extracts by correlation optimization warping in conjunction with  
571 pca, support vector machines and random forest data modeling. *Analytica Chimica Acta*.  
572 2009;642:257-65.
- 573 [37] Archer KJ, Kimes RV. Empirical characterization of random forest variable importance  
574 measures. *Computational Statistics & Data Analysis*. 2008;52:2249-60.
- 575 [38] Grömping U. Variable importance assessment in regression: Linear regression versus random  
576 forest. *The American Statistician*. 2009;63:308-19.
- 577 [39] Suykens JAK, Gestel TV, Brabanter JD, Moor BD, Vandewalle J. *Least squares support vector  
578 machines*. Singapore: World Scientific; 2002.
- 579 [40] Hsu C, Chang C, Lin C. *A practical guide to support vector classification*. 2010.
- 580 [41] Hastie T, Tibshirani R, Friedman J. *The elements of statistical learning: Data mining, inference  
581 and prediction*. 2 ed: Springer; 2009.
- 582 [42] Koo KY, Brownjohn JMW, List D, Cole R. Innovative structural health monitoring for  
583 suspension bridges by total positioning system. in *IABMAS10*. Philadelphia, USA. 2009.
- 584 [43] Westgate R, Brownjohn JMW. Development of a tamar bridge finite element model. in *IMAC  
585 XXVIII*. Florida, USA. 2010.
- 586 [44] Koo KY, Brownjohn JMW, Cole R, List DI. Structural health monitoring of tamar suspension  
587 bridge. Submitted to *Journal of Structural Control and Health Monitoring*. 2011.
- 588 [45] Koo KY, Brownjohn JMW. Robotic total station for long-term structural health monitoring of  
589 the tamar bridge. Submitted to *Engineering Structures*. 2011.
- 590 [46] Ni YQ, Zhou HF, Ko JM. Generalization capability of neural network models for temperature-  
591 frequency correlation using monitoring data: ASCE; 2009.
- 592 [47] Freund RJ, Wilson WJ, Mohr D. *Statistical methods*. London: Academic Press; 2010.
- 593 [48] Chao Y-CE, Zhao Y, Kupper LL, Nylander-French LA. Quantifying the relative importance of  
594 predictors in multiple linear regression analyses for public health studies. *Journal of  
595 Occupational and Environmental Hygiene*. 2008;5:519 - 29.
- 596 [49] Groemping U. Relative importance for linear regression in r: The package relaimpo. *Journal of  
597 Statistical Software*. 2006;17.
- 598
- 599
- 600
- 601

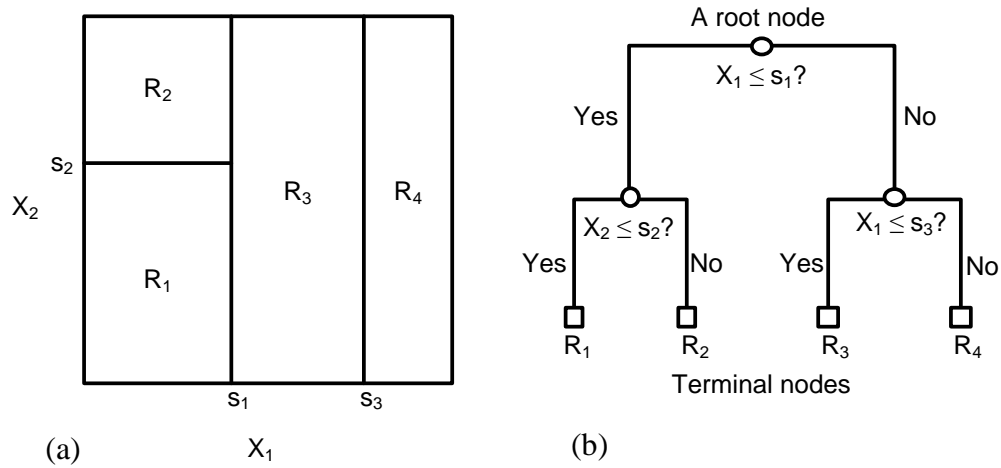


Figure 1. (a) The partitioning of a two-dimensional feature space into four regions,  $R_1$ - $R_4$ ; (b) a decision tree with three splits and four terminal nodes corresponding to the four partitions.

602  
 603  
 604

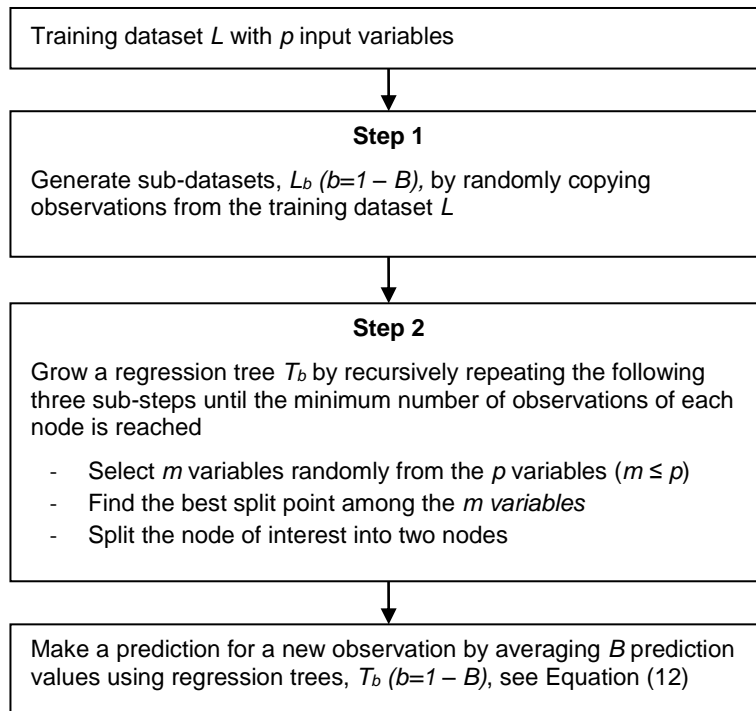


Figure 2. A layout of the random forest analysis method.

605

606



Figure 3. The Tamar Suspension Bridge

607

608

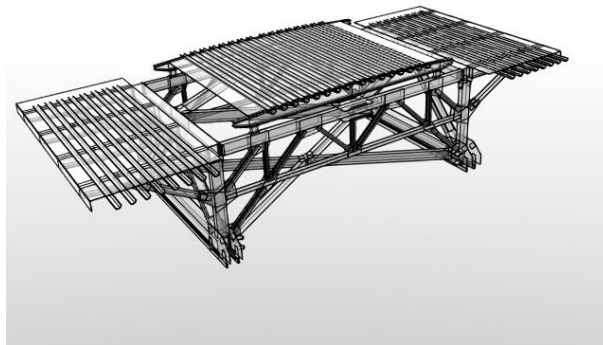


Figure 4 The truss section with the main orthotropic deck and two cantilever lanes

609

610

611

612

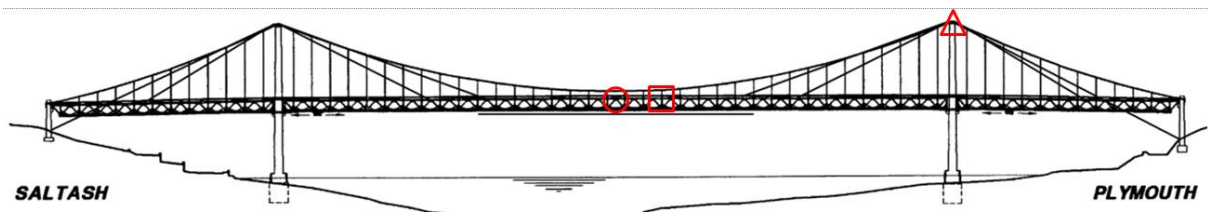


Figure 5 Sensor locations (circle for accelerometers, square for thermistors and triangle for anemometer)

613  
614  
615

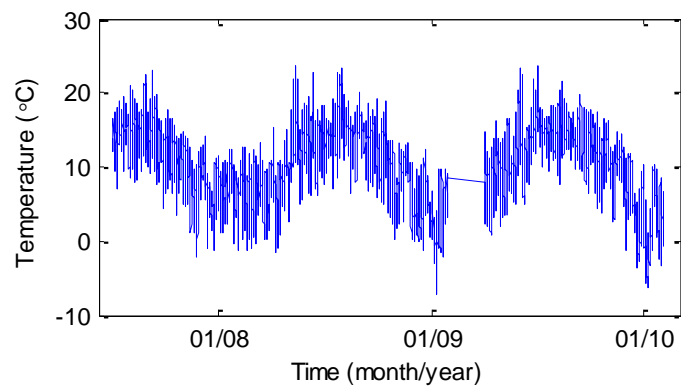


Figure 6. Time history of temperature measured from 2007 to 2010

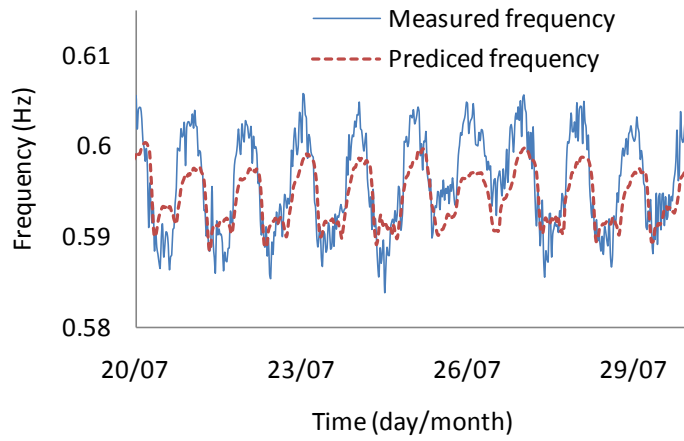


Figure 7. Measured and predicted natural frequencies between July 20 and July 30, 2009 using the multiple linear regression method.

616

617

618

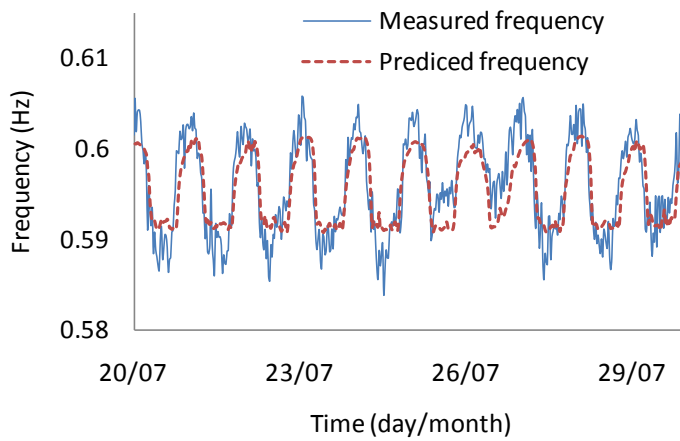


Figure 8. Measured and predicted natural frequencies between July 20 and July 30, 2009 using the artificial neural network method.

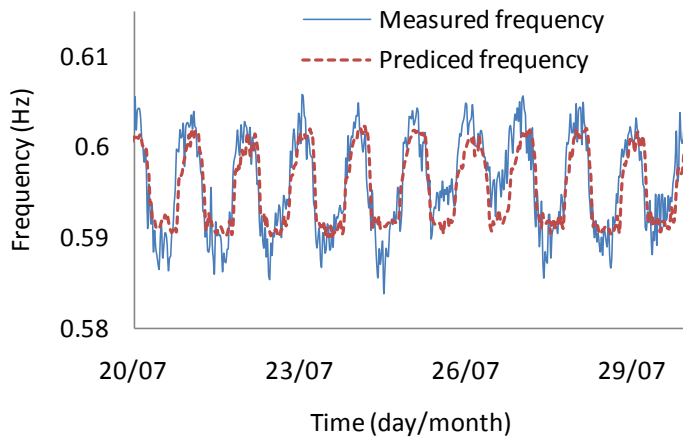


Figure 9. Measured and predicted natural frequencies between July 20 and July 30, 2009 using the support vector regression method.

619

620

621

622

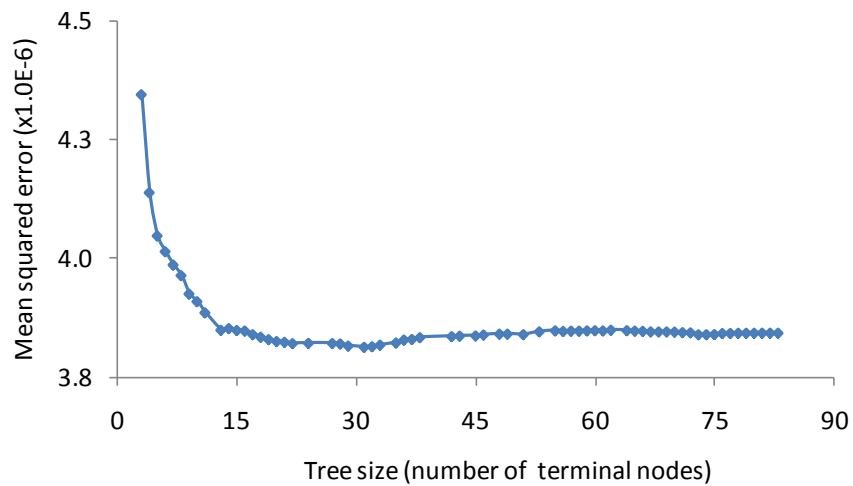


Figure 10. Mean squared errors versus the number of terminal nodes of a tree.

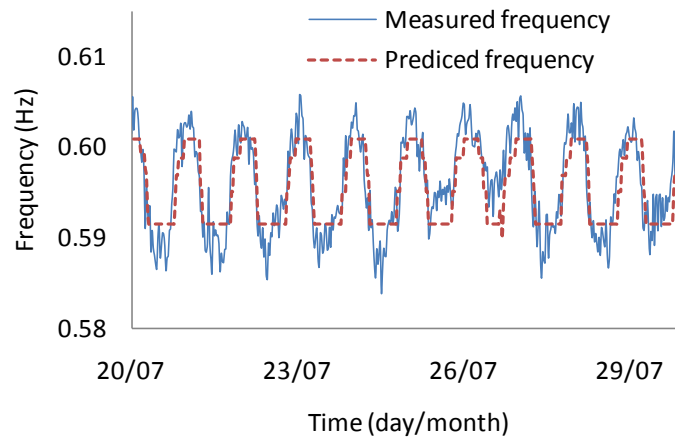


Figure 11. Measured and predicted natural frequencies between July 20 and July 30, 2009 using the regression tree method.

623

624

625

626

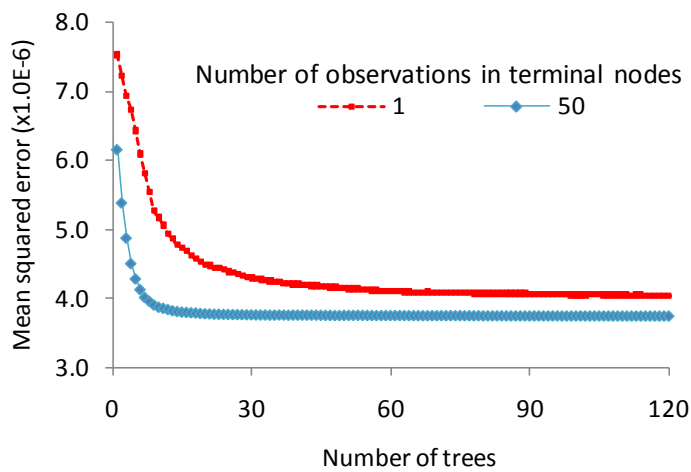


Figure 12. Mean squared errors versus number of trees for two cases of 1 and 50 observations in terminal nodes.

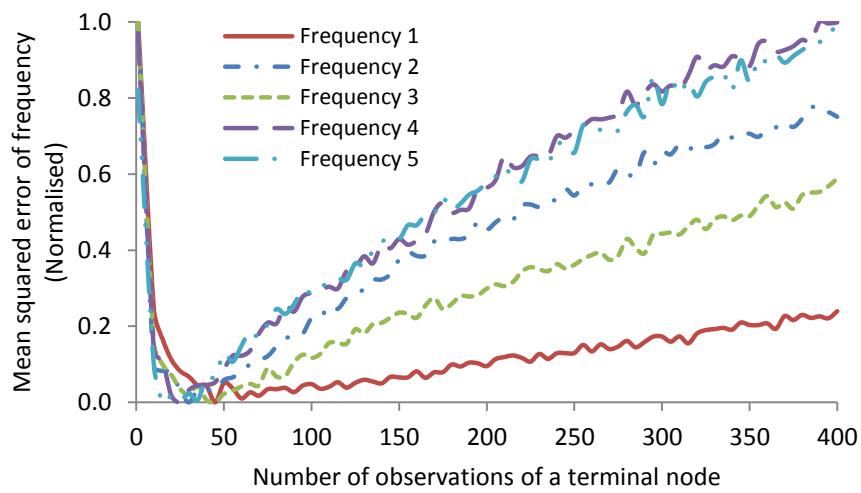


Figure 13. Mean squared errors versus the number of observations in a terminal node

627

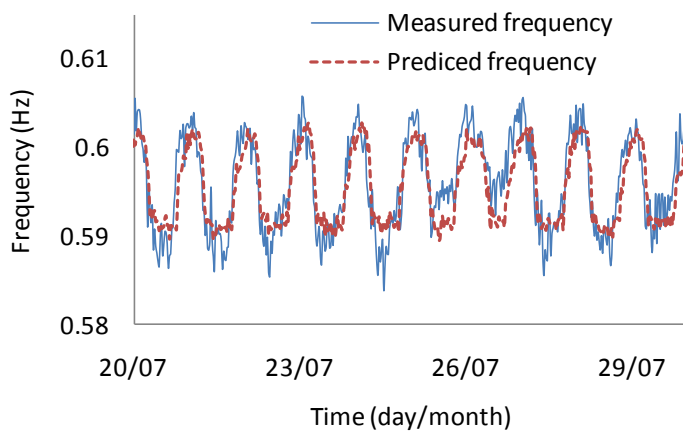


Figure 14. Measured and predicted natural frequencies between July 20 and July 30, 2009 using the random forest method

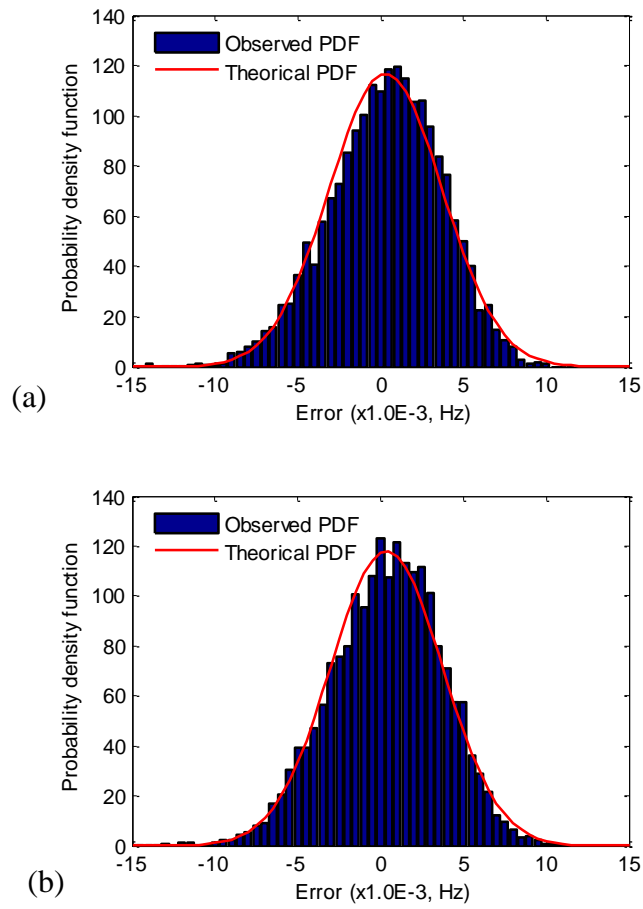


Figure 15. Probability distribution of errors for (a) support vector regression and (b) random forest

628

629

630

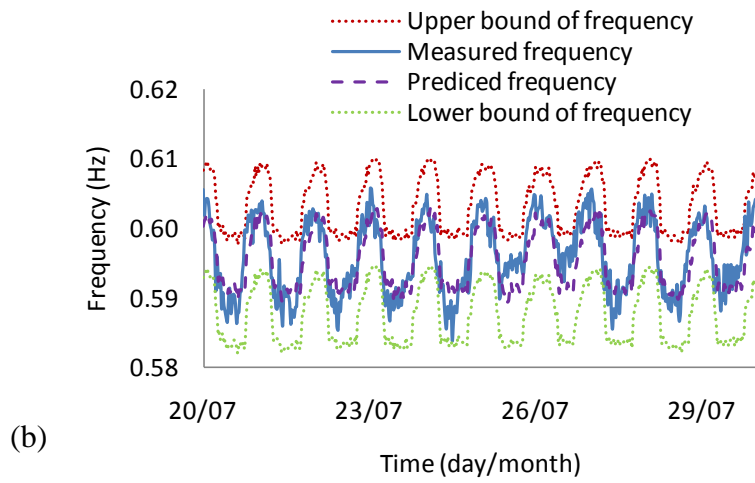
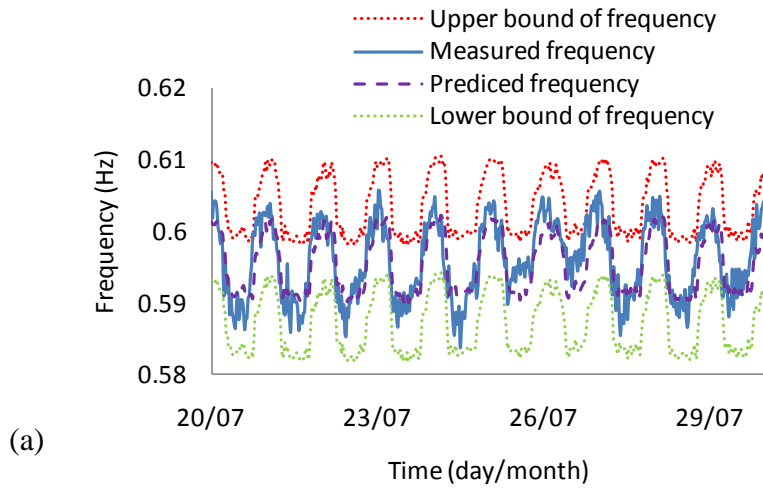


Figure 16. Measured and predicted natural frequencies (20 – 30 July, 2009) together with the 95% confidence interval using (a) support vector regression and (b) random forest

631

632

633

634

635

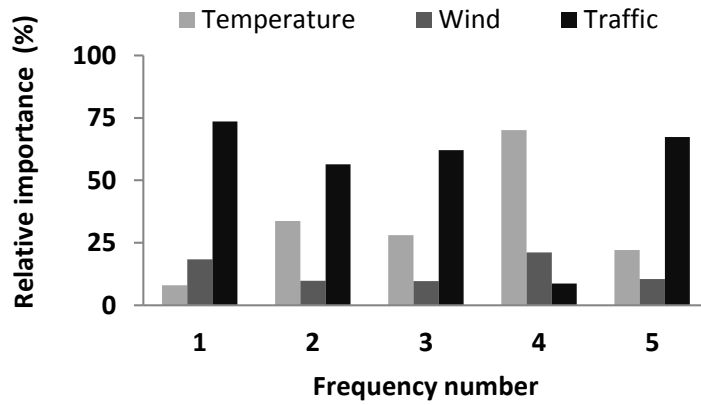


Figure 17. Evaluating simultaneous effects of temperature, wind, and traffic loading on the natural frequency responses through the relative importance of variables using the MLR method.

636  
637  
638  
639

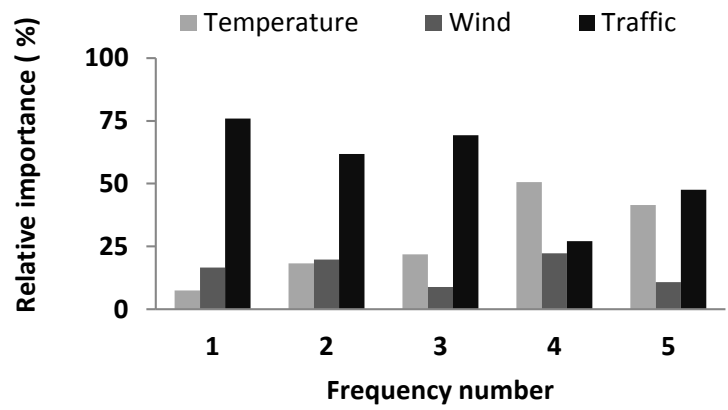


Figure 18. Evaluating simultaneous effects of temperature, wind, and traffic loading on the modal frequency responses through the relative importance of variables using the RF method.

640

641

Table 1. Parameters of measured natural frequencies of the bridge.

Mode number	Average frequency (Hz)	Frequency range (Hz)		Maximum difference (%)	Standard deviation (Hz)
		minimum	maximum		
1	0.39	0.38	0.41	8	0.00
2	0.47	0.41	0.57	34	0.01
3	0.60	0.58	0.61	5	0.01
4	0.69	0.67	0.70	4	0.00
5	0.73	0.71	0.75	6	0.01

642

643

644

645

Table 2. Results of the MLR method for the first five modes of the bridge

Frequency number	Mean squared error ( $\times 10^{-6}$ )	
	Training set	Test set
1	4.0	2.8
2	84.4	99.1
3	20.5	13.7
4	11.7	11.6
5	18.5	23.1

646

647

648

Table 3. Results of the ANN method for the first five modes of the bridge

Frequency number	Number of hidden nodes	Mean squared error ( $\times 10^{-6}$ )	
		Training set	Test set
1	11	3.9	2.7
2	10	87.6	95.7
3	21	22.8	12.3
4	33	15.7	18.6
5	21	19.5	20.0

649

650

651

Table 4. Results of the SVR method for the first five modes of the bridge

Frequency number	$\gamma$	$\alpha$	Mean squared error ( $\times 10^{-6}$ )	
			Training set	Test set
1	20	0.8	3.7	2.5
2	9	0.17	69.5	96.7
3	20	0.56	16.6	11.8
4	12	0.28	9.4	10.6
5	14	0.36	15.7	18.6

652

653

654

655

656

Table 5. Results of the R\_Tree method for the first five modes of the bridge

Frequency number	Number of terminal nodes	Mean squared error ( $\times 10^{-6}$ )	
		Training set	Test set
1	31	3.7	2.6
2	44	74.1	98.1
3	35	17.1	11.7
4	54	9.7	10.8
5	78	16.4	19.4

657

658

659

660

Table 6. Results of the RF method for the first five modes of the bridge

Frequency number	The optimal number of observations in terminal nodes	Mean squared error ( $\times 10^{-6}$ )	
		Training set	Test set
1	45	3.5	2.5
2	30	68.8	96.7
3	45	15.2	11.4
4	25	9.1	10.1
5	15	13.6	18.4

661

662

663

664

Table 7. Reduction in prediction errors of the ANN, SVR, R\_Tree and RF methods when using the prediction error of the MLR method as a basis.

665

666

Frequency number	Error reduction (%)			
	ANN*	SVR	R_Tree	RF
1	6.5	10.8	9.8	12.9
2	3	2.4	1.1	2.4
3	10.4	14.2	14.9	17.0
4	8.6	8.5	6.9	12.9
5	13.5	19.4	15.8	20.1

667

(\*) The error reduction for ANN when compared with the error of MLR,  $MSE_{MLR}$ , is equal to

668

$(MSE_{ANN} - MSE_{MLR}) \times 100 / MSE_{MLR}$ ; the same formulation is also applied for SVR, R\_Tree and

669

RF.